Influence of krypton physisorption on the positron surface state lifetime: rates of positron trapping into cavities



1990 J. Phys.: Condens. Matter 2 2081

(http://iopscience.iop.org/0953-8984/2/8/014)

J. Phys.: Condens. Matter 2 (1990) 2081–2091. Printed in the UK

# Influence of krypton physisorption on the positron surface state lifetime: rates of positron trapping into cavities

Kjeld O Jensen†‡, M Eldrup†, S Linderoth§ and J H Evans‖

† Metallurgy Department, Risø National Laboratory, DK-4000 Roskilde, Denmark

‡ School of Physics, University of East Anglia, Norwich NR4 7TJ, UK¶

§ Laboratory of Applied Physics, Technical University of Denmark, DK-2800 Lyngby, Denmark

‖ Materials Development Division, Harwell Laboratory, Oxfordshire OX11 0RA, UK

Received 7 August 1989

**Abstract.** The influence of physisorbed krypton on the lifetime of positrons trapped at copper surfaces has been investigated, using bulk Cu samples containing Kr-filled micrometre-size cavities. A decrease in the trapped-positron lifetime with decreasing temperature is attributed to adsorption of Kr on the cavity surfaces, in accordance with recent theoretical results of Jensen and Nieminen. The results demonstrate that positrons are trapped at the cavity surfaces. In addition, the trapping of positrons into the cavities is shown to be limited both by their rate of diffusion in the bulk, and their rate of transition into the cavities. The transition rate and its temperature dependence are estimated.

## 1. Introduction

Experimental techniques based on the interaction of positrons with surfaces are increasingly being applied to metals and semiconductors. In particular, variable-energy positron beams (Schultz and Lynn 1988) are emerging as powerful tools for investigating the properties of clean and adsorbate-covered surfaces. In order to be able to extract information about adsorption from positron studies it is essential to determine the influence of adsorbant on positron surface properties such as the annihilation characteristics of surface-trapped positrons. It has been predicted theoretically (Jensen and Nieminen 1987, Nieminen and Jensen 1988) that clear changes in the surface state lifetimes occur when atomic species such as the alkali metals and rare gases are adsorbed on metal surfaces.

In the present work we made the first experimental confirmation of the decrease in lifetime induced by rare gas adsorption. This is done for the case of Cu with physisorbed Kr using conventional (bulk) lifetime measurements on Cu samples containing large Kr-filled cavities. The controlled preparation of the surface and detailed surface characterisation possible in positron beam studies of external surfaces is not possible for cavity

¶ Present address.

0953-8984/90/082081 + 11 $03.50 

surfaces. On the other hand, lifetime measurements can be done only with difficulty in conjunction with beam techniques. Furthermore, in beam studies, epithermal positrons and positronium (Ps) escaping the sample surface may complicate the measurements (Huomo *et al* 1987), while in bulk samples, trapping into the cavities will take place mainly after thermalisation of the positrons. This makes it possible to study the temperature dependence of positron trapping into vacancy clusters or into large cavities which in this connection may be taken to represent an external surface. These temperature dependences have been the subject of much discussion (see, e.g., Eldrup and Jensen (1987) and Britton *et al* (1989)). In the present work we find that trapping of positrons into large cavities is limited both by the positron diffusion to the cavity and the transition into it. The deduced rates are found to agree fairly well with the theoretical estimates of Nieminen and Oliva (1980), but are about two orders of magnitude lower than the recent beam results obtained by Britton *et al* (1989).

In the next section we give some experimental details, while section 3 presents the results of a scanning electron microscopy study of the samples as well as the results of the positron lifetime measurements. In section 4 the results are discussed in detail, while section 5 contains a brief conclusion. A brief, preliminary discussion of the present results has appeared in the proceedings of the Eighth International Conference on Positron Annihilation (Jensen *et al* 1989).

## 2. Experimental details

The samples were prepared from Cu originally containing about 3% Kr, produced by a combined sputter deposition and ion implantation method (Whitmell 1981). They were later subjected to a thermal annealing sequence (Jensen *et al* 1988) and the present measurements were carried out after the final anneal at 1328 K. Most of the krypton was released during the annealing, but at the highest temperatures the remaining Kr (~100 ppm) stabilises large Kr-filled cavities (Kr bubbles).

The positron lifetime measurements were performed in three different systems used for different temperature ranges. All measurements were made with a 13 $\mu$Ci $^{22}$Na source contained between two 0.5 mg cm$^{-2}$ Ni foils which were sandwiched between the two pieces of sample. Measurements in the range 15–300 K were made at the Technical University of Denmark using a closed-cycle He refrigerator for sample cooling. Measurements in the range 100–535 K were carried out at Risø National Laboratory—up to 350 K with the samples in a liquid-nitrogen cryostat, and above 300 K in a vacuum furnace. The two standard lifetime spectrometers used had time resolutions of about 250 ps and 265 ps full width at half maximum, respectively. In each system the temperature was varied in a non-systematic way. No thermal hysteresis effects were detected.

The time resolution functions of the spectrometers in the different systems were determined from reference spectra measured for annealed Cu samples mounted in the same sample holders and using the same source as for the Cu–Kr samples. The reference spectra were analysed with the RESOLUTION program (Kirkegaard *et al* 1981). The resolution curve was determined frequently during the period of measurements, and small variations with time taken into account in the data analysis.

The lifetime spectra for the Cu–Kr samples were analysed using the POSITRONFIT program (Kirkegaard *et al* 1981). A correction for positrons annihilating in the source and at surfaces was subtracted in the analysis. The correction consisted of two

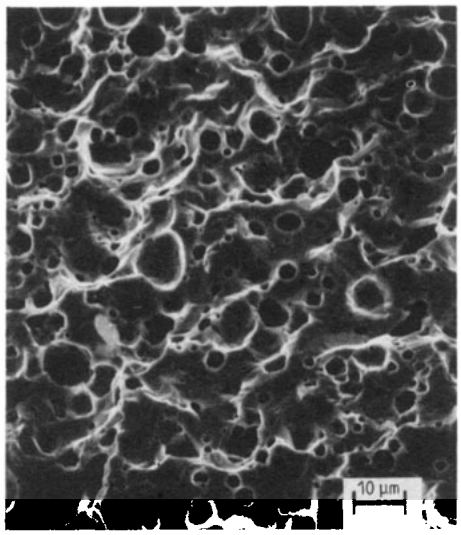


**Figure 1.** Scanning electron micrograph of the surface of one of the Cu (Kr) samples.

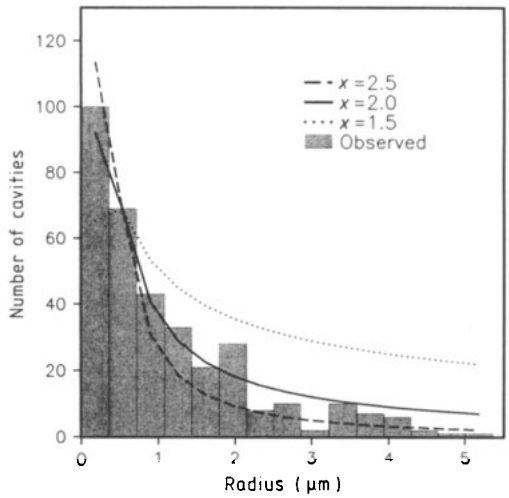


**Figure 2.** Distribution of radii observed on SEM micrographs of the Cu(Kr) sample surfaces (shaded histogram) compared to the estimated observed distributions calculated from equations (1) and (2) with $R_{low} = 0.2\,\mu m$ (curves). The values of the exponent $x$ are given in the figure.

components: one with a lifetime of 180 ps and 5% relative intensity (Linderoth *et al* 1984) due to annihilation in the Ni foils, and one with lifetime $\simeq$365 ps and intensity $\simeq$4% from source material and surfaces. The latter component was determined from the reference spectra and showed only a small variation with temperature.

## 3. Results

### *3.1. Scanning electron microscopy*

Scanning electron microscopy (SEM) of the surfaces of the annealed samples reveals a structure dominated by cavities with radii in the $\mu$m size range (see figure 1). The observed size distribution obtained from the SEM micrographs is shown as the histogram in figure 2. Apart from the statistical scatter, the number of cavities is particularly uncertain for the smallest radii, since cavities with radii smaller than about 0.2 $\mu$m are difficult to detect (also on micrographs with higher magnification than in figure 1).

The size distribution measured on the micrographs does not correspond to the true cavity size distribution, because the radius of the intersection of a cavity with the surface depends on the distance of the cavity centre from the surface, and because larger bubbles have larger probabilities of intersecting the surface. If we assume the cavities to be spherical and that the plane of the micrographs correspond to a random cross-section of the bulk structure it is straightforward to show that a true distribution $g(R)$ of radii $R$ gives rise to an observed distribution $f(r)$ of radii $r$ given by

$$f(r) = Ar \int_r^\infty g(R)(R^2 - r^2)^{-1/2}\,\mathrm{d}R \tag{1}$$

where $A$ is a normalisation constant.

A fair approximation to the measured cavity distribution can be obtained by assuming $g(R)$ to have the functional form given by

$$g(R) = \begin{cases} BR^{-x} & R > R_{\text{low}} \\ 0 & R < R_{\text{low}} \end{cases}. \tag{2}$$

The distribution $f(r)$ has been calculated with this $g(R)$ for three values of $x$. The three curves are shown in figure 2. Each point of the calculated distributions in figure 2 has been obtained by integrating equation (1) over the interval defined by the corresponding histogram column of the observed distribution.

$R_{\text{low}}$ was set to 0.2 $\mu$m and the constant $B$ has been adjusted to make the calculated distributions agree with the second point of the observed distribution for each of the three values of $x$ indicated in the figure. Comparing observed and calculated distributions shows that the distribution of cavity radii in the samples varies roughly as $R^{-2}$.

The density of Kr inside the cavities can be estimated from the equilibrium bubble condition (Greenwood *et al* 1959)

$$p = 2\gamma/R \tag{3}$$

which assumes that the force due to the gas pressure, $p$, inside the bubbles is balanced by the surface tension, $\gamma$. This relationship implies that the larger bubbles have lower pressures and thus Kr densities inside, and that the broad distribution of bubble sizes implies a similarly broad distribution of Kr densities being present in the cavities in the samples. With a value of 2 J m$^{-2}$ for $\gamma$ (Miedema 1978) and the ideal-gas equation of state (EOS), radii of 1–10 $\mu$m correspond to Kr densities in the bubbles of $2 \times 10^{25}$–$2 \times 10^{26}$ m$^{-3}$, if the bubbles have equilibrated at the annealing temperature of 1328 K which is a reasonable assumption due to the high concentration of thermal vacancies (Evans 1986). These estimates are consistent with a total Kr amount of the order of 100 at.ppm being distributed in the open volume calculated from the observed sample swelling of $\simeq$20% (Jensen *et al* 1988)

### 3.2. *Positron lifetime spectroscopy*

Two lifetime components were extracted from the measured spectra (apart from a $\simeq$2 ns lifetime and $\simeq$0.2% intensity component, probably related to the sample surfaces, which we shall not consider further). The two lifetimes, $\tau_1$ and $\tau_2$, and the intensity of the long-lived component, $I_2$, are shown as functions of temperature in figure 3. Estimates were made of the sensitivity of the data in figure 3 to systematic uncertainties, especially the observed small variations in the source–surface correction with temperature (see section 2). The largest changes of $\tau_2$ and $I_2$ induced by varying the source–surface correction correspond to only 1–2 times the size of the symbols in figure 3. Similarly, a careful search for a possible third lifetime component with a lifetime between $\tau_1$ and $\tau_2$ was carried out. Generally, only slightly better variance-of-fits were obtained by including the third component accompanied with a large, unsystematic scatter of intensities. Thus, we conclude that only two components can be reliably resolved. It is seen that this is done with good reproducibility for the different systems where the temperature ranges overlap.

The lifetime $\tau_1$ is seen to be nearly constant, showing a slight increase with temperature from 105 to 113 ps, in close agreement with the bulk Cu lifetime of 112 $\pm$ 2 ps

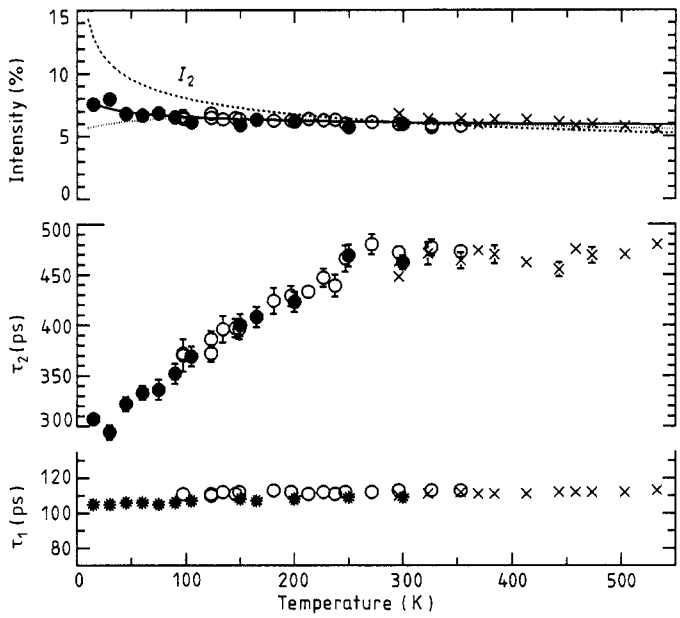


**Figure 3.** Results of a two-component analysis of lifetime spectra shown as function of measurement temperature. The three sets of symbols denote measurements made in each of the three systems used. Statistical uncertainties are shown when they are larger than the size of the symbols. The $I_2$ curves are calculated from equation (15) with three different choices for the transition rate parameter $\nu$; full curve: $\nu = (10^5 + 100\,T(\mathrm{K}))\ \mathrm{cm\ s^{-1}}$, dotted curve: $\nu = (10^5 + 2000\,T(\mathrm{K}))\ \mathrm{cm\ s^{-1}}$, broken curve: $\nu = \infty$.

at room temperature. This short-lived component is therefore believed to be due to non-trapped positrons.

The lifetime $\tau_2$ of the long-lived component is constant, equal to $470 \pm 10$ ps, at temperatures above $\simeq$250 K, while it decreases almost linearly at lower temperatures to reach about 300 ps at 15 K. The high-temperature value of $\tau_2$ is consistent with the values of about 500 ps reported for voids in Cu (Kögel *et al* 1979, Eldrup *et al* 1981). We therefore ascribe the long-lived component to positrons trapped in the cavities. The Kr densities estimated above are too low to affect the lifetime substantially, if the Kr is in the gas phase in the interior of the cavities (Jensen and Nieminen 1987). However, as discussed in detail in the next section, we interpret the decrease of $\tau_2$ at low temperatures as being due to the Kr as it adsorbs on the surfaces of the cavities.

The intensity $I_2$ decreases slightly with temperature, from about 7.5 to about 5.5%. This is much smaller than expected for purely diffusion limited trapping (the broken curve, figure 3). As discussed in detail below, the data show that the trapping is also limited by the transition into the cavities.

## 4. Discussion

### *4.1. Temperature variation of the positron lifetime*

In positron lifetime studies of voids, i.e. nominally empty cavities, no substantial changes of the lifetime as function of temperature are observed (see, e.g., Hyodo *et al* 1983,

Linderoth *et al* 1985, Eldrup and Jensen 1987). We therefore ascribe the temperature behaviour of $\tau_2$ to Kr present in the cavities, and we will, in particular, consider the effect of adsorption of Kr on the cavity surfaces.

It is easily shown that the amount of Kr in a bubble fulfilling the equilibrium condition, equation (3), is sufficient to form several full Kr layers at the bubble surfaces irrespective of the bubble size. Adsorption of a full monolayer of Kr is expected to decrease the lifetime of a surface-trapped positron from 500 ps to about 300 ps due to the annihilation of positrons with electrons from Kr atoms (Jensen and Nieminen 1987). Subsequent layers were found to have only a slight effect on the lifetime since these will be too far from the surface to affect the positron to any great extent. Thus, the absolute magnitude of the variation in $\tau_2$ with temperature (figure 3) is as expected from the theory. The fact that $\tau_2$ decreases approximately linearly with decreasing temperature is less readily accounted for but it can be done by considering the distribution of Kr densities in bubbles of different sizes (cf. section 3). We do this by constructing a model, described in the following, and by showing how this model can account for the observed results. Although the model relies on a number of simplifications, it incorporates the essential features of the physical system.

A thick (multi-layer) Kr film is condensed on the cavity surface when the temperature $T$ is lowered to the point where the Kr density, $n$, inside the cavity equals $p_{\text{vap}}(T)/kT$, where $p_{\text{vap}}$ is the Kr vapour pressure. However, at a given $n$, the first layer of Kr is adsorbed on the surface at a slightly higher $T$ than the thick-film condensation temperature. The Kr density $n_1$ at which a single adsorbed layer is formed can be written as:

$$n_1(T) = (p_0/kT)\exp(-q_{\text{st}}/kT) \tag{4}$$

where the prefactor $p_0$ and the isosteric heat of adsorption $q_{\text{st}}$ are parameters which can be obtained from surface adsorption experiments (Glachant *et al* 1982). Equation (4) follows from standard adsorption thermodynamics (Dash 1975) and the ideal-gas equation of state. The significance of equation (4) is that for a Kr density $n$ less than $n_1(T)$ no Kr is adsorbed at temperature $T$, while for $n \geq n_1(T)$ one or more Kr layers are present on the bubble surfaces. At low densities, the formation of the first adsorbed layer occurs as a sharp phase transition when $T$ is varied (Dash 1975, Pandit *et al* 1982, Glachant *et al* 1982, Unguris *et al* 1981). At higher densities the transition is no longer sharp and the formation of the Kr layers happens gradually over a finite temperature range (Dash 1975, Pandit *et al* 1982). However, for the purpose of the present qualitative model we assume the simpler picture outlined above to hold. We therefore assign a temperature-dependent lifetime $\tau(n, T)$ to a positron trapped by a bubble with Kr density $n$ given by

$$\tau(n, T) = \begin{cases} \tau_0 & n < n_1(T) \\ \tau_1 & n > n_1(T) \end{cases} \tag{5}$$

where $\tau_0$ and $\tau_1$ are the lifetimes when no Kr, and a full layer of Kr are adsorbed on the surface, respectively. Because of the small fraction of trapped positrons ($I_2 < 10\%$, see figure 3) only a single component with a lifetime determined by an average of the different lifetimes in the bubbles can be resolved. Equation (5) implies that the observed average bubble lifetime $\tau_b(T)$ is given by

$$\tau_b(T) = \tau_1 \int_{n_1(T)}^{\infty} \tilde{h}(n)\,\mathrm{d}n + \tau_0 \int_0^{n_1(T)} \tilde{h}(n)\,\mathrm{d}n \tag{6}$$

where $\tilde{h}(n)$ is the (normalised) distribution of Kr densities in the bubble population as

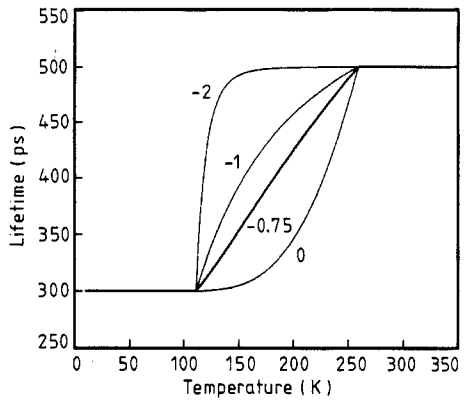


**Figure 4.** Variation of the average bubble positron lifetime calculated from the model described in the text. The parameter values are: $q_{st} = 0.13$ eV and $p_0 = 1.2$ GPa (Glachant *et al* 1982), $\tau_0 = 500$ ps, $\tau_1 = 300$ ps, $n_{low} = 10^{24}\,m^{-3}$, $n_{high} = 10^{27}\,m^{-3}$. The exponent $y$ is indicated for each curve. A linear dependence is obtained for $y = -0.75$ (highlighted).

sampled by the positrons. For simplicity we have ignored the temperature variation of $\tau_1$ due to thermal expansion of the Kr layer. Based on the measured expansion data for Kr layers (Unguris *et al* 1981), this effect can be estimated from the theory of Jensen and Nieminen (1987) to be only about 10 ps per 100 K and is therefore relatively unimportant in determining the overall shape of the $\tau_b$ versus $T$ curve. *A priori* we do not know the form of $\tilde{h}(n)$, but guided by the SEM data (section 3.1) we assume for the present calculations the simple form

$$\tilde{h}(n) = \begin{cases} Cn^y & n_{low} < n < n_{high} \\ 0 & \text{otherwise} \end{cases} \tag{7}$$

where $C$ is a constant. The results obtained for $\tau_b(T)$ are shown in figure 4. The parameters used in the calculations are given in the figure caption. It is seen that the behaviour observed experimentally (figure 3) is fairly well approximated for $y \simeq -0.75$. If the bubbles are in equilibrium, $n$ is proportional to $R^{-1}$ (equation (3)) and the bubble sizes detected by the positron are thus distributed as $h(R) = \tilde{h}(n_{eq}(R))/R^2$ where $n_{eq}(R) \propto R^{-1}$. For $\tilde{h}(n)$ proportional to $n^{-0.75}$ this means that $h(R)$ is proportional to $R^{-1.25}$. If the positron trapping probability $p(R)$ is proportional to $R^2$ (see section 4.2), the bubble size distribution derived from the positron results, $g(R) = h(R)/p(R)$, is therefore proportional to $R^{-3.25}$. This is in reasonable agreement with the approximate $R^{-2}$ distribution obtained from the SEM data (see figure 2), considering the approximations employed in both determinations of the distribution and the fact that the positron results depend on a much larger size range than observed by SEM.

The assumed upper and lower limits of the density distribution, and hence of the size distribution, determine the end-points of the slopes in the curves shown in figure 4. The $n_{high}$ value used in figure 4, corresponding via the equilibrium bubble relation to a radius of 0.2 $\mu$m, reproduces the experimental upper end-point temperature of 250 K. The existence of a lower end-point of the slope in figure 3 is less clear and it is therefore difficult to assign an upper limit to the size distribution based on the positron data. The $n_{low}$ value used in figure 4 of $10^{24}\,m^{-3}$, corresponding to an equilibrium radius of $\simeq$200 $\mu$m, gives a lower end-point around 110 K. However, the experimental value of $\tau_2$ continues to fall below this temperature. This could indicate that cavities even larger than 200 $\mu$m are present in the samples or that the Kr density in some cavities are below the density expected for equilibrium bubbles.

A complication, not considered so far, is that a positron may not trap directly into the surface state when it is trapped by a cavity, even when this state is the lowest-energy state of the system. Instead the positron may initially be emitted into the interior of the cavity, either as a free positron or as a Ps atom. In a small cavity, $R < 1\ \mu m$, this is fairly unimportant since the emission velocities of the positron or Ps atom of the order of $10^5\ m\ s^{-1}$ (deduced from positron and Ps emission spectra for Cu surfaces; see Howell *et al* (1985) and Murray *et al* (1980)) mean that the time taken to traverse the cavity is small compared to positron lifetimes. The positron will thus interact frequently with the surfaces and presumably rapidly make the transition into the surface state. For larger cavities, however, the effect could be appreciable because of the longer traverse times, and the effect of the adsorbed Kr on the positron and Ps emission probabilities and velocities might influence the variation of the observed lifetime with temperature. We will not attempt to evaluate these effects but only note that, if they are significant, they will only be prominent in the $\tau_b$ versus $T$ curve at low $T$, where the adsorption transition occurs in the large bubbles with low Kr density.

It has been demonstrated that the model presented above can account for the essential features of the experimental data. We have not attempted to make detailed quantitative comparisons, e.g. by letting some of the parameters be determined by a fit to the data, because of the extent of the assumptions and approximations in the model, although it is clear that better agreement could be obtained by adjusting some parameters, e.g. by setting $\tau_0 \simeq 475$ ps and $\tau_1 \simeq 325$ ps. The important points to notice are that the magnitude of the variation in lifetime between the lowest and highest temperatures is as expected from theory (Jensen and Nieminen 1987) and that the variation of $\tau_2$ below 250 K can be explained by a distribution of bubble sizes extending over several orders of magnitude (although the shape of the actual distribution may deviate from equation (7)) with Kr densities consistent with the equilibrium bubble condition.

### *4.2. Positron trapping into cavities*

As mentioned above, the $\tau_2$, $I_2$ component is associated with positrons trapped in the large cavities in the sample. In this section we discuss the magnitude and the variation with temperature of the intensity $I_2$ by constructing a model to calculate this quantity.

The large size of the cavities means that the positron trapping can be modelled using a plane-surface approximation. If the initial positron distribution perpendicular to a (planar) surface is given by $n_0(z)$, solution of the positron diffusion equation yields that the probability of escape through the surface is given by

$$P = \int_0^\infty dz\, n_0(z) \frac{\exp[-z/(D_+ \tau_{\text{eff}})^{1/2}]}{1 + \nu^{-1}(D_+/\tau_{\text{eff}})^{1/2}} \tag{8}$$

(Lynn 1981, Nieminen and Oliva 1980). $D_+$ is the positron diffusion constant and $\tau_{\text{eff}}$ is the effective bulk lifetime:

$$\tau_{\text{eff}} = (\lambda_b + \kappa)^{-1} \tag{9}$$

where $\lambda_b$ is the intrinsic bulk annihilation rate and $\kappa$ is the trapping rate into bulk defects.

The quantity $\nu$ in equation (8) is the total transition rate of all processes removing positrons from the bulk. It enters via the boundary condition

$$D_+(\delta/\delta z)n(z,t)|_{z=0} = \nu\, n(z=0,t) \tag{10}$$

where $n(z,t)$ is the (time-dependent) positron distribution (Nieminen and Oliva 1980). The positrons injected into the samples will, after thermalisation, initially be distributed uniformly in the material between cavities. The normalised (three-dimensional) positron density is

$$n_+ = [1 - N(4\pi/3)\langle R^3\rangle]^{-1} \tag{11}$$

where $N$ is the cavity density, $R$ the cavity radius, and $\langle R^3\rangle$ the average over the cavity distribution:

$$\langle R^3\rangle = \int_0^\infty \mathrm{d}R\, R^3 g(R). \tag{12}$$

To get the one-dimensional density perpendicular to the surface of a cavity of radius $R$, the 3D density is multiplied by the surface area. Thus

$$n_0(z) = \{4\pi R^2/[1 - N(4\pi/3)\langle R^3\rangle]\}. \tag{13}$$

Inserted into equation (8) this gives the probability $P(R)$ of trapping into a cavity of radius $R$:

$$P(R) = \{4\pi R^2/[1 - N(4\pi/3)\langle R^3\rangle]\}[1/(D_+\tau_{\mathrm{eff}})^{1/2} + 1/\nu\tau_{\mathrm{eff}}]^{-1}. \tag{14}$$

Averaging over the cavity size distribution and multiplying by the cavity density then gives the trapping probability (which is approximately equal to the intensity of the cavity component in a positron lifetime spectrum)

$$P = \int_0^\infty \mathrm{d}R\, P(R)g(R) = \frac{4\pi\langle R^2\rangle}{1/N - (4\pi/3)\langle R^3\rangle}\left(\frac{1}{(D_+\tau_{\mathrm{eff}})^{1/2}} + \frac{1}{\nu\tau_{\mathrm{eff}}}\right)^{-1}$$
$$= \frac{3\langle R^2\rangle}{\langle R^3\rangle}\left(\frac{1}{S} - 1\right)^{-1}\left(\frac{1}{(D_+\tau_{\mathrm{eff}})^{1/2}} + \frac{1}{\nu\tau_{\mathrm{eff}}}\right)^{-1} \tag{15}$$

where $S$ is the sample swelling, $S = N(4\pi/3)\langle R^3\rangle$.

Equation (15) can be used to predict the magnitude and temperature dependence of the cavity component intensity. Only a rough estimate can be made of the absolute magnitude because the cavity size distribution and thus $N$, $\langle R^2\rangle$ and $\langle R^3\rangle$ are poorly known, but the temperature dependence arises through $D_+$ and $\nu$ only and is thus independent of the cavity sizes.

The positron diffusion constant at room temperature is found both experimentally and theoretically to be about 1 $\mathrm{cm^2\,s^{-1}}$ (Schultz and Lynn 1988, Soininen *et al* 1989) and recent positron beam experiments (Huomo and co-workers 1987, 1989) support the $T^{-1/2}$ temperature dependence predicted when phonon scattering is the dominant scattering mechanism (McMullen 1985). Assuming, as above, that the surfaces of the large cavities can be considered equivalent to external planar surfaces, the transition rate $\nu$ is a sum of two terms (Nieminen and Oliva 1980, Britton *et al* 1989), $\nu = \nu_s + \nu_0$, $\nu_s$ representing the direct transition from the bulk into the surface state and $\nu_0$ Ps and free positron emission (in cavities with subsequent transition into the surface state, as discussed above). Nieminen and Oliva (1980) have estimated $\nu_s$ to be about $10^5$ $\mathrm{cm\,s^{-1}}$,

while Britton *et al* (1989) estimate a value 100 times higher. Measurements of branching ratios for positron surface processes (see Schultz and Lynn 1988) show that $\nu_0$ is of a magnitude similar to $\nu_s$. Theoretically, $\nu_0$ has been predicted to increase with temperature (from $\nu_0 = 0$ for $T = 0$) (Nieminen and Oliva 1980, Britton *et al* 1989). Recently, this has been demonstrated also experimentally (Britton *et al* 1989).

We have evaluated $P$ from equation (15) using a simple linear temperature dependence of $\nu$, as derived by Nieminen and Oliva (1980): $\nu = \nu_s + \alpha T$. For the diffusion constant we used $D_+ = (T/300\ \mathrm{K})^{-1/2} \times 1\ \mathrm{cm^2\ s^{-1}}$ and took $\tau_{\mathrm{eff}}$ equal to the bulk lifetime of 112 ps. This implies an assumption of no trapping into bulk defects which is justified by the temperature dependence of $\tau_1$ (figure 3). The near constancy of $\tau_1$ in the whole temperature range, equal to the lifetime for bulk copper, gives no indication of trapping into, e.g., shallow traps at low temperatures. With $S = 0.2$ and $\langle R^3\rangle/\langle R^2\rangle$ of about 1 $\mu$m, equation (15) gives absolute values of $P$ at 300 K in the range 3–8% for all reasonable values of $\nu$ (see below), in accordance with the experimental $I_2$ (figure 3). The temperature dependence of $P$ (equation 15) was calculated for a number of parameter sets ($\nu_s$, $\alpha$) and compared to the experimental $I_2$ (figure 3). Because of the rather large uncertainties on the absolute values, the calculated curves were scaled to agree with experiments at 300 K. It turns out that for a range of correlated values of $\nu_s$ and $\alpha$ almost equally good fits to the data were obtained, i.e. for ($\nu_s$, $\alpha$) in the range ($0.5 \times 10^5\ \mathrm{cm\ s^{-1}}$, 0) to ($1.7 \times 10^5\ \mathrm{cm\ s^{-1}}$, $700\ \mathrm{cm\ s^{-1}\ K^{-1}}$), the best being for $\nu_s = 10^5\ \mathrm{cm\ s^{-1}}$, $\alpha = 100\ \mathrm{cm\ s^{-1}\ K^{-1}}$. This is illustrated in figure 3 by three curves: the full curve is for the best fit just mentioned. The broken curve is for $\nu = \infty$, equivalent to a perfectly absorbing surface which means that the trapping is purely diffusion limited. The dotted curve shows the dependence predicted by Nieminen and Oliva (1980), $\nu_s = 10^5\ \mathrm{cm\ s^{-1}}$, $\alpha = 2000\ \mathrm{cm\ s^{-1}\ K^{-1}}$.

The real temperature dependence of $\nu$ may be more complicated than a simple linear form. However, the present data does not allow us to examine the detailed temperature behaviour, and it is unlikely that using a more elaborate form will yield absolute values for $\nu$ significantly different from those presented above.

It is clearly seen that the case of a perfectly absorbing surface ($\nu = \infty$) predicts a temperature dependence ($T^{-1/4}$) which is much stronger than observed. Only the cases with finite $\nu$ reproduce the experimental data reasonably well. The $\nu_s$ value obtained agrees closely with the estimate of Nieminen and Oliva (1980) while the best fit is obtained for a temperature dependence of $\nu$ which is weaker than their prediction. A value of $10^7\ \mathrm{cm\ s^{-1}}$ as obtained by Britton *et al* (1989) would mean that $\nu\tau_{\mathrm{eff}}$ were much larger than $(D_+\tau_{\mathrm{eff}})^{1/2}$ (equation 15) at all temperatures above 10 K and would thus give results very close to those for purely diffusion limited trapping ($\nu = \infty$, figure 3) which is clearly not consistent with the present results.

## 5. Conclusions

The results of the present investigation of positron behaviour in copper containing $\mu$m-size krypton-filled cavities are two-fold. First, the variation of the lifetime of positrons trapped in the cavities is shown to be a result of Kr adsorption at low temperatures at the cavity surfaces, where the trapped positrons are localised. Secondly, the trapping of the positrons into the cavities is shown to be limited both by the positron diffusion to the cavities and by the rate of transition through the surface into the cavities. The transition

rate can be described by $\nu = \nu_s + \alpha T$, with $\nu_s = (1.1 \pm 0.6) \times 10^5$ cm s$^{-1}$ and $\alpha = 0$–700 cm s$^{-1}$ K$^{-1}$.

## Acknowledgments

The authors wish to thank D Britton and A Vehanen for discussions and N J Pedersen for competent technical assistance. One of us (KOJ) would like to thank the Science and Engineering Research Council for a research associateship.

## References

Britton D T, Huttunen P A, Mäkinen J, Soininen E and Vehanen A 1989 *Phys. Rev. Lett.* **62** 2413
Dash J G 1975 *Films on Solid Surfaces* (New York: Academic)
Eldrup M, Evans J H, Mogensen O E and Singh B N 1981 *Radiat. Eff.* **54** 65
Eldrup M and Jensen K O 1987 *Phys. Status Solidi* a **102** 145
Evans J H 1986 *Nucl. Instrum. Methods* B **18** 16
Glachant A, Jaubert M, Bienfait M and Boato G 1982 *Surf. Sci.* **115** 219
Greenwood G W, Foreman A J E and Rimmer D E 1959 *J. Nucl. Mater.* **4** 305
Howell R H, Meyer P, Rosenberg I J and Fluss M J 1985 *Phys. Rev. Lett.* **54** 1698
Huomo H, Soininen E and Vehanen A 1989 (submitted for publication)
Huomo H, Vehanen A, Bentzon M D and Hautojärvi P 1987 *Phys. Rev.* B **35** 8252
Hyodo T, Douglas R J, Grynszpan R, McKee B T A and Stewart A T 1983 *J. Phys. F: Met. Phys.* **13** 573
Jensen K O, Eldrup M, Linderoth S and Evans J H 1989 *Positron Annihilation* ed L Dorikens-Vanpraet, M Dorikens and D Segers (Singapore: World Scientific) p 345
Jensen K O, Eldrup M, Pedersen N J and Evans J H 1988 *J. Phys. F: Met. Phys.* **18** 1703
Jensen K O and Nieminen R M 1987 *Phys. Rev.* B **36** 8219
Kirkegaard P, Eldrup M, Mogensen O E and Pedersen N J 1981 *Comput. Phys. Commun.* **23** 307
Kögel G, Winter J and Triftshäuser W 1979 *Positron Annihilation* ed Hasiguti R R and Fujiwara K (Sendai: Japan Institute of Metals) p 707
Linderoth S, Bentzon M D, Hansen H E and Petersen K 1985 *Positron Annihilation* ed P C Jain *et al* (Singapore: World Scientific) p 494
Linderoth S, Hansen H E, Nielsen B and Petersen K 1984 *Appl. Phys.* A **33** 25
Lynn K G 1981 *Positron Solid-State Physics* ed W Brandt and A Dupasquier (Amsterdam: North-Holland) p 609
McMullen T 1985 *Positron Annihilation* ed P C Jain *et al* (Singapore: World Scientific) p 657
Miedema A R 1978 *Z. Metallk.* **69** 287
Murray C A, Mills A P and Rowe J E 1980 *Surf. Sci.* **100** 647
Nieminen R M and Jensen K O 1988 *Phys. Rev.* B **38** 5764
Nieminen R M and Oliva J 1980 *Phys. Rev.* B **22** 2226
Pandit R, Schick M and Wortis M 1982 *Phys. Rev.* B **26** 5112
Schultz P J and Lynn K G 1988 *Rev. Mod. Phys.* **60** 701
Soininen E, Huomo H, Huttunen P, Mäkinen J, Vehanen A and Hautojärvi P 1989 (submitted for publication)
Unguris J, Bruch L W, Moog E R and Webb M B 1981 *Surf. Sci.* **109** 522
Whitmell D S 1981 *Radiat. Eff.* **53** 209